Computational Methods for Compressible Flow

Learning Objectives

After reading this handout and participating in classroom lectures and discussion, students will be able to

- Recognize the compressible Navier-Stokes equations.
- Describe three important physical differences between compressible and incompressible flow and the implications that these differences have for computation.
- Derive a generic one-dimensional finite-volume formulation for inviscid compressible flow.
- Describe two approaches to flux evaluation for compressible flow, including the underlying physical reasoning behind the schemes.
- Describe boundary conditions for the compressible Euler equations.

1 Compressible Navier-Stokes Equations

As we've discussed at great length already, the incompressible Navier-Stokes equations consist of two momentum equations, with auxiliary equations for the conservation of momentum and of energy. These equations can be written in conservation-law form in three dimensions

as:

$$\begin{aligned}
\frac{\partial u}{\partial x}+\frac{\partial v}{\partial y}+\frac{\partial w}{\partial z} &= 0 \\
\frac{\partial u}{\partial t}+\frac{\partial u^2}{\partial x}+\frac{\partial uv}{\partial y}+\frac{\partial uw}{\partial z} &= -\frac{1}{\rho}\frac{\partial P}{\partial x}+\frac{\mu}{\rho}\nabla^2 u \\
\frac{\partial v}{\partial t}+\frac{\partial uv}{\partial x}+\frac{\partial v^2}{\partial y}+\frac{\partial vw}{\partial z} &= -\frac{1}{\rho}\frac{\partial P}{\partial y}+\frac{\mu}{\rho}\nabla^2 v \\
\frac{\partial w}{\partial t}+\frac{\partial uw}{\partial x}+\frac{\partial vw}{\partial y}+\frac{\partial w^2}{\partial z} &= -\frac{1}{\rho}\frac{\partial P}{\partial z}+\frac{\mu}{\rho}\nabla^2 w \\
\frac{\partial T}{\partial t}+\frac{\partial uT}{\partial x}+\frac{\partial vT}{\partial y}+\frac{\partial wT}{\partial z} &= \frac{k}{\rho c_p}\nabla^2 T \\
&\quad +\frac{\mu}{\rho c_p}\left(2\left(\frac{\partial u}{\partial x}\right)^2+2\left(\frac{\partial v}{\partial y}\right)^2+2\left(\frac{\partial w}{\partial z}\right)^2\right. \\
&\quad \left.+\left(\frac{\partial u}{\partial z}+\frac{\partial w}{\partial x}\right)^2+\left(\frac{\partial v}{\partial x}+\frac{\partial u}{\partial y}\right)^2+\left(\frac{\partial w}{\partial y}+\frac{\partial v}{\partial z}\right)^2\right)
\end{aligned} \tag{1}$$

The equations are more complex for compressible flow, because the density varies with pressure and temperature. This in turn implies more complicated expressions for transport of mass and momentum by convection, and also makes it more convenient to solve directly for energy instead of for temperature. This results in the following set of equations.[1]

$$\begin{aligned}
\frac{\partial \rho}{\partial t}+\frac{\partial \rho u}{\partial x}+\frac{\partial \rho v}{\partial y}+\frac{\partial \rho w}{\partial z} &= 0 \\
\frac{\partial \rho u}{\partial t}+\frac{\partial \rho u^2}{\partial x}+\frac{\partial \rho uv}{\partial y}+\frac{\partial \rho uw}{\partial z} &= -\frac{\partial P}{\partial x}+\frac{\partial}{\partial x}\tau_{xx}+\frac{\partial}{\partial y}\tau_{xy}+\frac{\partial}{\partial z}\tau_{xz} \\
\frac{\partial \rho v}{\partial t}+\frac{\partial \rho uv}{\partial x}+\frac{\partial \rho v^2}{\partial y}+\frac{\partial \rho vw}{\partial z} &= -\frac{\partial P}{\partial y}+\frac{\partial}{\partial x}\tau_{yx}+\frac{\partial}{\partial y}\tau_{yy}+\frac{\partial}{\partial z}\tau_{yz} \\
\frac{\partial \rho w}{\partial t}+\frac{\partial \rho uw}{\partial x}+\frac{\partial \rho vw}{\partial y}+\frac{\partial \rho w^2}{\partial z} &= -\frac{\partial P}{\partial z}+\frac{\partial}{\partial x}\tau_{zx}+\frac{\partial}{\partial y}\tau_{zy}+\frac{\partial}{\partial z}\tau_{zz} \\
\frac{\partial E_t}{\partial t}+\frac{\partial u(E_t+P)}{\partial x}+\frac{\partial v(E_t+P)}{\partial y}+\frac{\partial w(E_t+P)}{\partial z} &= \frac{\partial}{\partial x}\left(u\tau_{xx}+v\tau_{xy}+w\tau_{xz}-q_x\right) \\
&\quad +\frac{\partial}{\partial y}\left(u\tau_{yx}+v\tau_{yy}+w\tau_{yz}-q_y\right) \\
&\quad +\frac{\partial}{\partial z}\left(u\tau_{zx}+v\tau_{zy}+w\tau_{zz}-q_z\right)
\end{aligned} \tag{2}$$

[1] The derivation of these equations can be found in any good compressible flow textbook.

where the energy E represents the total thermal and kinetic energy of the gas.

$$E_t = \rho C_v T + \rho \frac{u^2 + v^2 + w^2}{2} \tag{3}$$

$$P = \rho R T \tag{4}$$

$$c = \sqrt{\gamma R T} = \sqrt{\frac{\gamma P}{\rho}} \tag{5}$$

$$\vec{q} = -k \nabla T \tag{6}$$

$$\tau = \mu \begin{bmatrix} 2\frac{\partial u}{\partial x} - \frac{2}{3}\nabla \cdot \vec{u} & \frac{\partial u}{\partial y} + \frac{\partial v}{\partial x} & \frac{\partial u}{\partial z} + \frac{\partial w}{\partial x} \\ \frac{\partial u}{\partial y} + \frac{\partial v}{\partial x} & 2\frac{\partial v}{\partial y} - \frac{2}{3}\nabla \cdot \vec{u} & \frac{\partial v}{\partial z} + \frac{\partial w}{\partial y} \\ \frac{\partial u}{\partial z} + \frac{\partial w}{\partial x} & \frac{\partial v}{\partial z} + \frac{\partial w}{\partial y} & 2\frac{\partial w}{\partial z} - \frac{2}{3}\nabla \cdot \vec{u} \end{bmatrix} \tag{7}$$

The definition of speed of sound, c, has been introduced (Eq 5), along with the equation of state (Eq. 3), and the perfect gas law (Eq. 4). Note that the shear stress tensor is traceless; in tensor notation, this is written as

$$\tau = \mu \left(S + S^T - \frac{2}{3} \text{trace } S \right)$$

where the strain rate tensor S has components $S_{ij} = \frac{\partial u_i}{\partial x_j}$. Physically, this amounts to folding the mean viscous normal stress into the pressure term. Equations 2 can be re-written in two dimensions and in divergence form as

$$\frac{\partial U}{\partial t} + \frac{\partial F}{\partial x} + \frac{\partial G}{\partial y} = 0 \tag{8}$$

where

$$U = \begin{pmatrix} \rho \\ \rho u \\ \rho v \\ E_t \end{pmatrix} \tag{9}$$

$$F = \begin{pmatrix} \rho u \\ \rho u^2 + P - \tau_{xx} \\ \rho uv - \tau_{xy} \\ u\left(E_t + P - \tau_{xx}\right) - v\tau_{xy} + q_x \end{pmatrix} \tag{10}$$

$$G = \begin{pmatrix} \rho v \\ \rho uv - \tau_{yx} \\ \rho v^2 + P - \tau_{yy} \\ -u\tau_{yx} + v\left(E_t + P - \tau_{yy}\right) + q_y \end{pmatrix} \tag{11}$$

There are several noteworthy differences between the physics of compressible as opposed to incompressible flow. While we won't delve deeply into the details of these differences here, we will hit some of the points that affect the way in which we discretize the equations.

Non-constant density. For compressible flow, the density depends on the pressure and temperature rather than being constant. Physically, this variation of density allows mass to be stored within a control volume, which has the effect of adding a term to the continuity equation that reflects the rate of change of mass in the control volume $\left(\frac{\partial \rho}{\partial t}\right)$.

Continuity and energy fully coupled with momentum. Because the density, pressure, and temperature are all interrelated, it is no longer appropriate to solve the energy equation separately from the momentum equations. Generally the pressure is computed from temperature and density using the perfect gas law. Density has its own conservation equation, and temperature is computed from the energy and the equation of state when needed.

Furthermore, because conservation of mass, momentum, and energy are strongly coupled, all the conservation equations are solved simultaneously. The fluxes and Jacobians can be assembled for use with approximate factorization or Gauss-Seidel line relaxation schemes, or with GMRES, just as the incompressible "continuity" and momentum equations were.

Finite propagation speed for pressure disturbances. Pressure waves travel at finite speed in compressible flow (mathematically hyperbolic), whereas in incompressible flow, pressure changes are theoretically propagated instantaneously (mathematically elliptic). The finite speed of pressure (acoustic) waves for compressible flow allows us to use upwind discretization for all parts of inviscid compressible flow if we wish.

1.1 Non-Dimensionalization of the Compressible Governing Equations

Just as for incompressible flow, we typically prefer to solve these equations in non-dimensional form. The dimensional form has variables that range over five orders of magnitude in SI units: density is $1.2\,{}^{\mathrm{kg}}/_{\mathrm{m}^3}$ and pressure is $10^5\,\mathrm{Pa}$ at sea level. This variation in values can introduce numerical stiffness into the problem. Also, working with non-dimensional variables makes it easier to change flow conditions to match a different Mach and Reynolds number.

To non-dimensionalize the compressible flow equations, we need reference quantities for density, length, and velocity. For density and velocity, we typically choose far-field values of

density and speed of sound for external flows. For internal flows, some other reference flow condition must be used. So we have:

$$\begin{aligned}
\rho &= \rho^* \rho_\infty \\
\vec{x} &= \vec{x}^* L \\
\vec{V} &= \vec{V}^* c_\infty \\
t &= t^* L / c_\infty \\
P &= P^* \rho_\infty c_\infty^2 \\
T &= T^* \frac{c_\infty^2}{\gamma R}
\end{aligned}$$

Substituting these into the compressible Navier-Stokes equations and pulling out all the constants, we get:

$$\frac{\rho_\infty c_\infty}{L}\left\{\frac{\partial \rho^*}{\partial t^*} + \frac{\partial \rho^* u^*}{\partial x^*} + \frac{\partial \rho^* v^*}{\partial y^*} + \frac{\partial \rho^* w^*}{\partial z^*}\right\} = 0$$

$$\frac{\rho_\infty c_\infty^2}{L}\left\{\frac{\partial \rho^* u^*}{\partial t^*} + \frac{\partial \rho^* u^{*^2}}{\partial x^*} + \frac{\partial \rho^* u^* v^*}{\partial z^*} + \frac{\partial \rho^* u^* w^*}{\partial z^*}\right\} = -\frac{\rho_\infty c_\infty^2}{L}\frac{\partial P^*}{\partial x^*} + \frac{1}{L}\left(\frac{\partial}{\partial x^*}\tau_{xx}^* + \frac{\partial}{\partial y^*}\tau_{xy}^* + \frac{\partial}{\partial z^*}\tau_{xz}^*\right) \quad (12)$$

$$\frac{\rho_\infty c_\infty^2}{L}\left\{\frac{\partial \rho^* v^*}{\partial t^*} + \frac{\partial \rho^* u^* v^*}{\partial x^*} + \frac{\partial \rho^* v^{*^2}}{\partial z^*} + \frac{\partial \rho^* v^* w^*}{\partial z^*}\right\} = -\frac{\rho_\infty c_\infty^2}{L}\frac{\partial P^*}{\partial y^*} + \frac{1}{L}\left(\frac{\partial}{\partial x^*}\tau_{yx}^* + \frac{\partial}{\partial y^*}\tau_{yy}^* + \frac{\partial}{\partial z^*}\tau_{yz}^*\right) \quad (13)$$

$$\frac{\rho_\infty c_\infty^2}{L}\left\{\frac{\partial \rho^* u^*}{\partial t^*} + \frac{\partial \rho^* u^* w^*}{\partial x^*} + \frac{\partial \rho^* v^* w^*}{\partial z^*} + \frac{\partial \rho^* w^{*^2}}{\partial z^*}\right\} = -\frac{\rho_\infty c_\infty^2}{L}\frac{\partial P^*}{\partial z^*} + \frac{1}{L}\left(\frac{\partial}{\partial x^*}\tau_{zx}^* + \frac{\partial}{\partial y^*}\tau_{zy}^* + \frac{\partial}{\partial z^*}\tau_{zz}^*\right) \quad (14)$$

$$\begin{aligned}
\frac{\rho_\infty c_\infty^3}{L}\left\{\frac{\partial E_t^*}{\partial t^*} + \frac{\partial u^*(E_t^*+P^*)}{\partial x^*} + \frac{\partial v^*(E_t^*+P^*)}{\partial y^*} + \frac{\partial w^*(E_t^*+P^*)}{\partial z^*}\right\} &= \frac{c_\infty}{L}\frac{\partial}{\partial x^*}\left(u^*\tau_{xx}^* + v^*\tau_{xy}^* + w^*\tau_{xz} - \frac{q_x^*}{c_\infty}\right) \\
&+ \frac{c_\infty}{L}\frac{\partial}{\partial y^*}\left(u^*\tau_{yx}^* + v^*\tau_{yy}^* + w^*\tau_{yz} - \frac{q_y^*}{c_\infty}\right) \\
&+ \frac{c_\infty}{L}\frac{\partial}{\partial z^*}\left(u^*\tau_{zx}^* + v^*\tau_{zy}^* + w^*\tau_{zz} - \frac{q_z^*}{c_\infty}\right)
\end{aligned}$$

where (after some simplification),

$$E_t^* = \frac{1}{\gamma(\gamma-1)}\rho^* T^* + \rho^* \frac{u^{*^2} + v^{*^2} + w^{*^2}}{2}$$

$$P^* = \frac{\rho^* T^*}{\gamma}$$

$$c^* = \sqrt{T^*} = \sqrt{\frac{\gamma P^*}{\rho^*}}$$

$$\vec{q}^* = -\frac{k c_\infty^2}{\gamma R L}\nabla^* T^*$$

$$\tau = \frac{\mu}{\mu_\infty}\frac{\mu_\infty c_\infty}{L}\begin{bmatrix} 2\frac{\partial u^*}{\partial x^*} - \frac{2}{3}\nabla^*\cdot\vec{u}^* & \frac{\partial u^*}{\partial y^*} + \frac{\partial v^*}{\partial x^*} & \frac{\partial u^*}{\partial z^*} + \frac{\partial w^*}{\partial x^*} \\ \frac{\partial u^*}{\partial y^*} + \frac{\partial v^*}{\partial x^*} & 2\frac{\partial v^*}{\partial y^*} - \frac{2}{3}\nabla^*\cdot\vec{u}^* & \frac{\partial v^*}{\partial z^*} + \frac{\partial w^*}{\partial y^*} \\ \frac{\partial u^*}{\partial z^*} + \frac{\partial w^*}{\partial x^*} & \frac{\partial v^*}{\partial z^*} + \frac{\partial w^*}{\partial y^*} & 2\frac{\partial w^*}{\partial z^*} - \frac{2}{3}\nabla^*\cdot\vec{u}^* \end{bmatrix}$$

where γ is the ratio of specific heats and μ_∞ is the viscosity evaluated at the reference temperature T_∞; μ/μ_∞ captures the temperature variation of viscosity. The viscous stress terms in the x-momentum equation can be written as:

$$\begin{aligned}\frac{L}{\rho_\infty c_\infty^2}\frac{1}{L}\left(\frac{\partial}{\partial x^*}\tau_{xx}^* + \frac{\partial}{\partial y^*}\tau_{xy}^* + \frac{\partial}{\partial z^*}\tau_{xz}^*\right) =& \frac{\mu}{\mu_\infty}\frac{U_\infty}{c_\infty}\frac{\mu_\infty}{\rho_\infty U_\infty L}\left(\frac{\partial}{\partial x^*}\left(2\frac{\partial u^*}{\partial x^*} - \frac{2}{3}\nabla^*\cdot\vec{u}^*\right)\right. \\ &\left. + \frac{\partial}{\partial y^*}\left(\frac{\partial u^*}{\partial y^*} + \frac{\partial v^*}{\partial x^*}\right) + \frac{\partial}{\partial z^*}\left(\frac{\partial u^*}{\partial z^*} + \frac{\partial w^*}{\partial x^*}\right)\right)\end{aligned}$$

or, to express τ^* directly,

$$\tau^* = \frac{\tau}{\rho_\infty c_\infty^2} = \frac{\mu}{\mu_\infty}\frac{1}{M_\infty Re_\infty}\begin{bmatrix} 2\frac{\partial u^*}{\partial x^*} - \frac{2}{3}\nabla^*\cdot\vec{u}^* & \frac{\partial u^*}{\partial y^*} + \frac{\partial v^*}{\partial x^*} & \frac{\partial u^*}{\partial z^*} + \frac{\partial w^*}{\partial x^*} \\ \frac{\partial u^*}{\partial y^*} + \frac{\partial v^*}{\partial x^*} & 2\frac{\partial v^*}{\partial y^*} - \frac{2}{3}\nabla^*\cdot\vec{u}^* & \frac{\partial v^*}{\partial z^*} + \frac{\partial w^*}{\partial y^*} \\ \frac{\partial u^*}{\partial z^*} + \frac{\partial w^*}{\partial x^*} & \frac{\partial v^*}{\partial z^*} + \frac{\partial w^*}{\partial y^*} & 2\frac{\partial w^*}{\partial z^*} - \frac{2}{3}\nabla^*\cdot\vec{u}^* \end{bmatrix}$$

The heat flux in the x-direction can be written as

$$\begin{aligned}\frac{L}{\rho_\infty c_\infty^3}\frac{c_\infty}{L}\frac{\partial}{\partial x^*}\frac{q_x^*}{c_\infty} &= -\frac{1}{\rho_\infty c_\infty^3}\frac{\partial}{\partial x^*}\left(\frac{k c_\infty^2}{\gamma R L}\frac{\partial T^*}{\partial x^*}\right) \\ &= -\frac{k}{\gamma\rho_\infty R c_\infty L}\frac{k_\infty}{k_\infty}\frac{\mu_\infty}{\mu_\infty}\frac{\partial^2 T^*}{\partial x^{*^2}} \\ &= -\frac{1}{M_\infty Re_\infty}\frac{k}{k_\infty}\frac{k_\infty}{(\gamma-1)c_p\mu_\infty}\frac{\partial^2 T^*}{\partial x^{*^2}} \\ &= -\frac{1}{Pr_\infty M_\infty Re_\infty}\frac{k}{k_\infty}\frac{1}{\gamma-1}\frac{\partial^2 T^*}{\partial x^{*^2}}\end{aligned}$$

or, to express $\vec{q}^*$ directly,

$$\vec{q}^* = -\frac{\vec{q}}{\rho_\infty c_\infty^3} = \frac{1}{Pr_\infty Re_\infty}\frac{k}{k_\infty}\frac{1}{\gamma-1}\nabla^* T^*$$

Just as we did for the incompressible N-S equations, we note that the form of the equations is the same, and we drop all the *'s. Finally, putting all of this back together, we get

$$\begin{aligned}
\frac{\partial \rho}{\partial t} + \frac{\partial \rho u}{\partial x} + \frac{\partial \rho v}{\partial y} + \frac{\partial \rho w}{\partial z} &= 0 \\
\frac{\partial \rho u}{\partial t} + \frac{\partial \rho u^2}{\partial x} + \frac{\partial \rho uv}{\partial y} + \frac{\partial \rho uw}{\partial z} &= -\frac{\partial P}{\partial x} + \frac{\partial \tau_{xx}}{\partial x} + \frac{\partial \tau_{xy}}{\partial y} + \frac{\partial \tau_{xz}}{\partial z} \\
\frac{\partial \rho v}{\partial t} + \frac{\partial \rho uv}{\partial x} + \frac{\partial \rho v^2}{\partial y} + \frac{\partial \rho vw}{\partial z} &= -\frac{\partial P}{\partial y} + \frac{\partial \tau_{yx}}{\partial x} + \frac{\partial \tau_{yy}}{\partial y} + \frac{\partial \tau_{yz}}{\partial z} \\
\frac{\partial \rho w}{\partial t} + \frac{\partial \rho uw}{\partial x} + \frac{\partial \rho vw}{\partial y} + \frac{\partial \rho w^2}{\partial z} &= -\frac{\partial P}{\partial z} + \frac{\partial \tau_{zx}}{\partial x} + \frac{\partial \tau_{zy}}{\partial y} + \frac{\partial \tau_{zz}}{\partial z} \\
\frac{\partial E_t}{\partial t} + \frac{\partial u(E_t+P)}{\partial x} + \frac{\partial v(E_t+P)}{\partial y} + \frac{\partial w(E_t+P)}{\partial z} &= \frac{\partial}{\partial x}\left(u\tau_{xx} + v\tau_{xy} + w\tau_{xz} - q_x\right) \\
&\quad + \frac{\partial}{\partial y}\left(u\tau_{yx} + v\tau_{yy} + w\tau_{yz} - q_y\right) \\
&\quad + \frac{\partial}{\partial z}\left(u\tau_{zx} + v\tau_{zy} + w\tau_{zz} - q_z\right)
\end{aligned} \tag{15}$$

with

$$\begin{aligned}
E_t &= \frac{1}{\gamma(\gamma-1)}\rho T + \rho\frac{u^2+v^2+w^2}{2} \\
P &= \frac{\rho T}{\gamma} \\
c &= \sqrt{T} = \sqrt{\frac{\gamma P}{\rho}} \\
\vec{q} &= -\frac{1}{Pr_\infty M_\infty Re_\infty}\frac{k}{k_\infty}\frac{1}{\gamma-1}\nabla T \\
\tau &= \frac{\mu}{\mu_\infty}\frac{1}{M_\infty Re_\infty}\begin{bmatrix} 2\frac{\partial u}{\partial x} - \frac{2}{3}\nabla\cdot\vec{u} & \frac{\partial u}{\partial y} + \frac{\partial v}{\partial x} & \frac{\partial u}{\partial z} + \frac{\partial w}{\partial x} \\ \frac{\partial u}{\partial y} + \frac{\partial v}{\partial x} & 2\frac{\partial v}{\partial y} - \frac{2}{3}\nabla\cdot\vec{u} & \frac{\partial v}{\partial z} + \frac{\partial w}{\partial y} \\ \frac{\partial u}{\partial z} + \frac{\partial w}{\partial x} & \frac{\partial v}{\partial z} + \frac{\partial w}{\partial y} & 2\frac{\partial w}{\partial z} - \frac{2}{3}\nabla\cdot\vec{u} \end{bmatrix}
\end{aligned}$$

2 Finite Volume Discretization of the Compressible Euler Equations

Before diving into the details of discretization of the compressible Euler equations, let's first develop a generic finite-volume space discretization for these equations in one dimension. We begin with the (dimensional) Navier-Stokes equations[2] and immediately neglect all viscous terms, leaving us with

$$\frac{\partial U}{\partial t} + \frac{\partial F}{\partial x} = 0$$

where

$$\begin{aligned} U &= \begin{pmatrix} \rho \\ \rho u \\ E_t \end{pmatrix} \\ F &= \begin{pmatrix} \rho u \\ \rho u^2 + P \\ u(E_t + P) \end{pmatrix} \\ E_t &= \rho c_v T + \rho \frac{u^2}{2} \\ P &= \rho R T \end{aligned}$$

Recasting this into control volume form, we have:

$$\left.\frac{\partial \bar{U}}{\partial t}\right|_i = -\frac{F_{i+\frac{1}{2}} - F_{i-\frac{1}{2}}}{\Delta x} \tag{16}$$

3 Flux Evaluation for the Compressible Euler Equations

Section 2 isn't exactly earth-shaking; it's just an application of finite-volume methods to the one-dimensional compressible Euler equations. The critical question, as always with finite volume methods, is how to evaluate the fluxes at control volume boundaries. We will discuss two methods for doing this, each of which has a physical interpretation in terms of characteristic theory.

[2]Yes, it's true: all the derivations are done for the dimensional equations, but the code is written for non-dimensional equations. This is mostly a matter of replacing the specific heats and gas constant with the proper expressions involving γ.

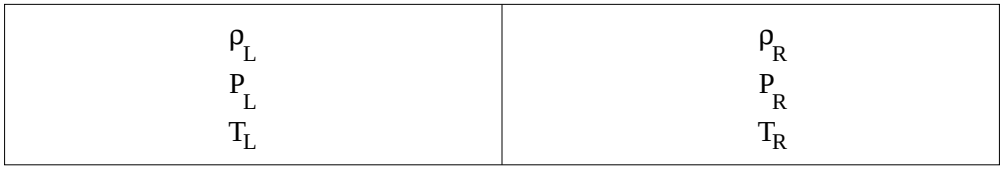

Figure 1: Shock tube problem

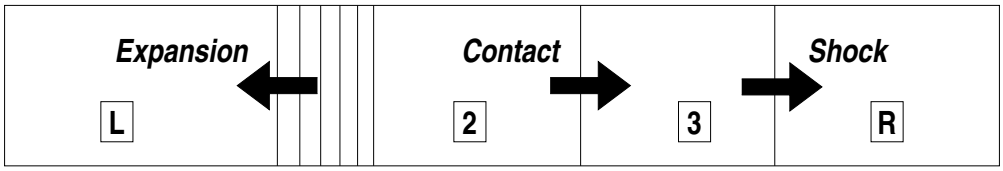

Figure 2: Wave pattern resulting from shock tube problem

To compare the relative merits of these methods, we will use each approach to solve a *Riemann* or *shock tube problem*, which is a classic test problem for one-dimensional compressible flow. Consider a straight tube of uniform cross-section divided into two sections by a membrane (see Figure 1). The two sections contain gas at different density, pressure, and temperature and at zero velocity. At time zero, the membrane ruptures. In the general case, a *compression wave* travels into the low pressure gas while an *expansion wave* travels into the high pressure gas. Also, a *contact discontinuity* is created, in general, marking the division between gas originally on the high-pressure side of the membrane and gas originally on the low-pressure side (see Figure 2); across the contact discontinuity, pressure and velocity remain constant, but the entropy (and therefore density and temperature) can change abruptly. Results for three test cases will be shown, each of which has zero velocity on both sides of the diaphragm and $\rho_R = P_R = 1$. These cases are therefore characterized by the values of ρ_L and P_L.

1. A stationary contact discontinuity: $\rho_L = 1.01$ and $P_L = 1$.
2. A weak pressure difference: $\rho_L = 1$ and $P_L = 1.01$.
3. A strong, moving shock: $\rho_L = 8$ and $P_L = 10$.

3.1 Flux-Vector Splitting (Steger-Warming)

For compressible flow, we know that all disturbances travel at a finite speed; that is, all disturbances are wave-like. This implies that we can decompose the flux into right-moving

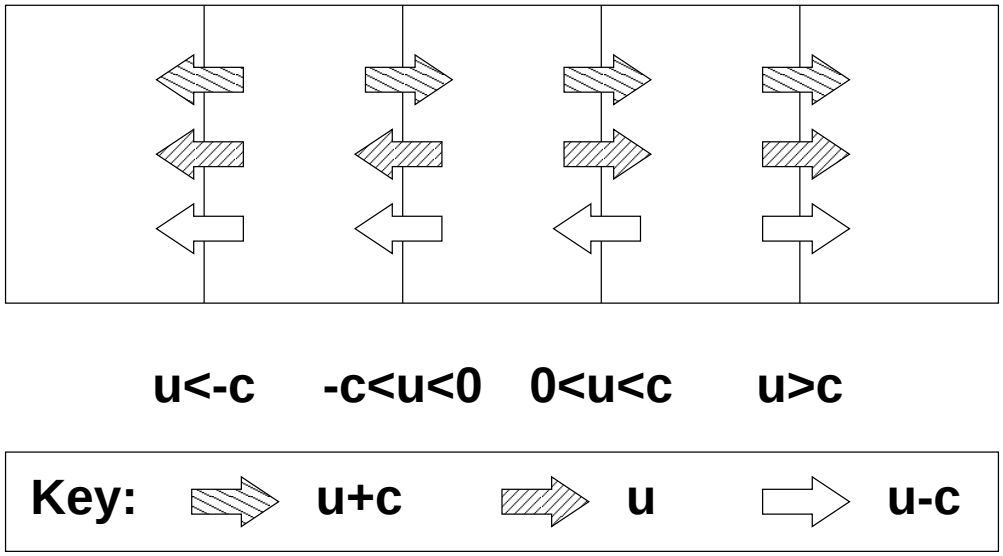

Figure 3: Flux upwinding using flux vector splitting

and left-moving components and approximate each component using only upwind data, as shown by example in Figure 3. This technique was first used by Steger and Warming and is known as *flux-vector splitting*.

To decompose the flux into right-moving and left-moving components, we appeal to *characteristic theory*. Mathematically, characteristic theory provides a way to find exact solutions of linear hyperbolic systems of equations. Although our problem is non-linear, we can still use characteristic theory (linearizing about some particular solution if need be). We begin by noting that, for the compressible Euler equations,

$$F = AU$$

as you can easily verify.[3] Our goal is to write $A = A^+ + A^-$ where A^+ is associated with right-moving waves and A^- with left-moving waves. Then we can approximate

$$F_{i+\frac{1}{2}} = \left(A^+U\right)_{i+\frac{1}{2};i} + \left(A^-U\right)_{i+\frac{1}{2};i+1}$$

where $U_{i+\frac{1}{2};i}$ is the reconstructed value of U just to the left of the interface and $U_{i+\frac{1}{2};i+1}$ is the reconstructed value of U just to the right of the interface.

[3]This is because $F(U)$ is a homogeneous function of U of degree 1. That is, the sum of the powers of the components of U in each term of $F(U)$ is 1.

Characteristic theory tells us that the eigenvalues[4] of A are the wave speeds for the hyperbolic system. Both for convenience and to facilitate physical interpretation of the eigenvectors, we apply a unitary transformation[5] on A, resulting in a matrix known to have the same eigenvalues but different eigenvectors. This transformation is

$$\hat{A} = \frac{\partial V}{\partial U} A \frac{\partial U}{\partial V} \tag{17}$$

where $V = (\rho \; u \; P)^T$. Then

$$A \equiv \frac{\partial F}{\partial U} = \begin{bmatrix} 0 & 1 & 0 \\ -u^2 \frac{3-\gamma}{2} & u(3-\gamma) & \gamma - 1 \\ -\gamma \frac{uE_t}{\rho} + (\gamma-1)u^3 & \gamma \frac{E_t}{\rho} - \frac{3(\gamma-1)}{2} u^2 & \gamma u \end{bmatrix} \tag{18}$$

$$\frac{\partial U}{\partial V} = \begin{bmatrix} 1 & 0 & 0 \\ u & \rho & 0 \\ \frac{u^2}{2} & \rho u & \frac{1}{\gamma - 1} \end{bmatrix} \tag{19}$$

$$\frac{\partial V}{\partial U} = \frac{\partial U}{\partial V}^{-1} = \begin{bmatrix} 1 & 0 & 0 \\ -\frac{u}{\rho} & \frac{1}{\rho} & 0 \\ (\gamma-1)\frac{u^2}{2} & -(\gamma-1)u & \gamma - 1 \end{bmatrix} \tag{20}$$

[4] A quick refresher on the relevant bits about eigenvalues and eigenvectors. Recall that the eigenvalues λ and right eigenvectors x_R of a matrix B are defined by

$$B x_R = \lambda x_R$$

while the left eigenvectors x_L are defined by

$$x_L B = \lambda x_L$$

Each eigenvector, both left and right, is unique to within a constant factor provided that the eigenvalues of the matrix are all distinct. Therefore, we can choose the constant factors so that the matrix X_L whose rows are the left eigenvectors x_L and the matrix X_R whose columns are the right eigenvectors x_R are inverses:

$$X_R = X_L^{-1}$$

Then we can diagonalize B by writing:

$$\begin{aligned} X_L B X_R &= X_L \left[\lambda_1 x_{R,1} \; \lambda_2 x_{R,2} \; \lambda_3 x_{R,3} \right] \\ &= \begin{bmatrix} \lambda_1 & & \\ & \lambda_2 & \\ & & \lambda_3 \end{bmatrix} \equiv \Lambda \end{aligned}$$

[5] That is, a transformation T for which $T^T T = T T^T = I$.

After some tedious but straightforward calculation, we can combine the above to get

$$\hat{A} = \begin{bmatrix} u & \rho & 0 \\ 0 & u & \frac{1}{\rho} \\ 0 & \gamma P & u \end{bmatrix} \tag{21}$$

The eigenvalues of $\hat{A}$ (and therefore also those of A) are found from the definition of eigenvalue:

$$\begin{aligned} \hat{A}x_R &= \lambda x_R \\ \left(\hat{A} - \lambda I\right) x_R &= 0 \end{aligned}$$

This last equation has solutions for non-trivial x_R if and only if the determinant of $\hat{A} - \lambda I$ is zero. Referring to Equation 21, we get the following equation for λ.

$$(u-\lambda)^3 - (u-\lambda)\frac{\gamma P}{\rho} = 0$$

which has $\lambda = u, u \pm c$ as solutions. Given these values of λ, the x_R are determined to within a constant factor. The constants can be chosen so that

$$X_R = \begin{bmatrix} \underline{(u)} & \underline{(u+c)} & \underline{(u-c)} \\ 1 & \frac{\rho}{c} & -\frac{\rho}{c} \\ 0 & 1 & 1 \\ 0 & \rho c & -\rho c \end{bmatrix} \tag{22}$$

and

$$X_L = \begin{bmatrix} (u): & 1 & 0 & -\frac{1}{c^2} \\ (u+c): & 0 & \frac{1}{2} & \frac{1}{2\rho c} \\ (u-c): & 0 & \frac{1}{2} & -\frac{1}{2\rho c} \end{bmatrix} \tag{23}$$

Note that $X_L V$ give the *invariants* for each wave; that is, the combination of quantities which is constant along an isolated wave of that type; this turns out to be convenient for implementing boundary conditions, as we will see.

Having dispensed with the preliminaries, we now come to the crux of flux-vector splitting. Note that, since $\hat{A} = X_R \Lambda X_L$, A can be written as

$$A = \frac{\partial U}{\partial V} X_R \Lambda X_L \frac{\partial V}{\partial U}$$

which means that

$$F = \frac{\partial U}{\partial V} X_R \Lambda X_L \frac{\partial V}{\partial U} U$$

This looks like a lot of work to compute something that we already know how to compute directly. But now we can decompose the flux F into components associated with the eigenvalues.

$$\begin{aligned}
F &= \frac{\partial U}{\partial V} X_R \begin{bmatrix} \lambda_1 & & \\ & \lambda_2 & \\ & & \lambda_3 \end{bmatrix} X_L \frac{\partial V}{\partial U} U \\
&= \frac{\partial U}{\partial V} X_R \begin{bmatrix} \lambda_1 & & \\ & 0 & \\ & & 0 \end{bmatrix} X_L \frac{\partial V}{\partial U} U \\
&+ \frac{\partial U}{\partial V} X_R \begin{bmatrix} 0 & & \\ & \lambda_2 & \\ & & 0 \end{bmatrix} X_L \frac{\partial V}{\partial U} U \\
&+ \frac{\partial U}{\partial V} X_R \begin{bmatrix} 0 & & \\ & 0 & \\ & & \lambda_3 \end{bmatrix} X_L \frac{\partial V}{\partial U} U
\end{aligned}$$

Now when we need to compute the flux at an interface $i+\frac{1}{2}$, we use the following procedure.

1. Compute the eigenvalues λ_k using averaged data at the control volume boundary:

$$\begin{aligned}
\lambda_1 &= \frac{u_{i+\frac{1}{2};i} + u_{i+\frac{1}{2};i+1}}{2} \\
\lambda_2 &= \frac{(u+c)_{i+\frac{1}{2};i} + (u+c)_{i+\frac{1}{2};i+1}}{2} \\
\lambda_3 &= \frac{(u-c)_{i+\frac{1}{2};i} + (u-c)_{i+\frac{1}{2};i+1}}{2}
\end{aligned}$$

   These eigenvalues can be used to determine what direction is upwind for each component of the flux; that is, to determine which terms in the expanded flux Jacobian, above, are calculated using data from which control volume. Alternatively, we can evaluate $\lambda_i^{\pm} = \frac{\lambda_i + |\lambda_i|}{2}$ for each eigenvalue in the upwinded flux expressions, below, using data from each side of the face separately. This can, in principle, result in more or less than three eigenvalues being active at a given face, but in those cases the speeds involved are so low that the flux error is also quite low.

2. In control volume i, compute the flux F_i^+ for all eigenvalues which are greater than 0 (right-moving waves) using data from the left side of the interface:

$$F_i^+ = \left(\frac{\partial U}{\partial V} X_R \Lambda^+ X_L \frac{\partial V}{\partial U} \right)_{U_{i+\frac{1}{2};i}} U_{i+\frac{1}{2};i}$$

where Λ^+ is a diagonal matrix whose non-zero entries are positive eigenvalues of A.

$$\Lambda^+ \equiv \frac{1}{2}\begin{bmatrix} u+|u| & 0 & 0 \\ 0 & u+c+|u+c| & 0 \\ 0 & 0 & u-c+|u-c| \end{bmatrix}$$

3. Similarly, in control volume $i+1$, compute the flux F^-_{i+1} for all eigenvalues which are less than zero (left-moving waves) using data from the right side of the interface:

$$F^-_{i+1} = \left(\frac{\partial U}{\partial V} X_R \Lambda^- X_L \frac{\partial V}{\partial U}\right)_{U_{i+\frac{1}{2};i+1}} U_{i+\frac{1}{2};i+1}$$

where Λ^- is a diagonal matrix whose non-zero entries are negative eigenvalues of A.

$$\Lambda^- \equiv \frac{1}{2}\begin{bmatrix} u-|u| & 0 & 0 \\ 0 & u+c-|u+c| & 0 \\ 0 & 0 & u-c-|u-c| \end{bmatrix}$$

4. Finally, $F_{i+\frac{1}{2}} = F^+_i + F^-_{i+1}$.

3.2 Flux-Difference Splitting (Roe's Scheme)

A major difficulty with the Steger-Warming flux-vector splitting scheme is that it is highly diffusive. The reason for this is that the Steger-Warming scheme always has non-zero fluxes at each control volume interface; a steady-state is achieved by balance of these fluxes. Roe's scheme avoids this problem by use a centered flux evaluation plus a diffusion term that amounts to splitting the *difference* of the fluxes on the left and right side of the control volume boundary into left-moving and right-moving components. This approach can be shown to project the difference of the fluxes onto the eigenvectors of a special Jacobian and upwind each of these flux components.

Roe's scheme computes the flux at a control volume boundary using the following flux function:

$$F_{i+\frac{1}{2}} = \frac{1}{2}\left(F_{i+\frac{1}{2};i} + F_{i+\frac{1}{2};i+1}\right) - \frac{1}{2}\left|\tilde{A}\right|\left(U_{i+\frac{1}{2};i+1} - U_{i+\frac{1}{2};i}\right) \tag{24}$$

where $F_{i+\frac{1}{2};i}$ is the normal Euler flux evaluated using $U_{i+\frac{1}{2};i}$ and

$$\begin{aligned} \tilde{A} &= \left(\frac{\partial U}{\partial V} X_R \Lambda X_L \frac{\partial V}{\partial U}\right)_{\tilde{U}} \\ |\tilde{A}| &= \left(\frac{\partial U}{\partial V} X_R |\Lambda| X_L \frac{\partial V}{\partial U}\right)_{\tilde{U}} \\ |\Lambda| &= \mathrm{diag}(|\lambda_1|, |\lambda_2|, |\lambda_3|) \end{aligned} \tag{25}$$

and $\tilde{A}(U_L, U_R)$ is chosen to represent local flow conditions well. Obvious candidates include $\tilde{A} = \frac{1}{2}(A_L + A_R)$ and $\tilde{A} = A(\frac{1}{2}(U_L + U_R))$. However, Roe's scheme requires that:

1. $\tilde{A}$ provides a linear mapping from the vector solution space (U) to the vector flux space (F).
2. As $U_R \to U_L \to U$, $\tilde{A}(U_L, U_R) \to A(U)$.
3. For any U_L, U_R, $\tilde{A}(U_L, U_R) \cdot (U_L - U_R) = F_L - F_R$.
4. The eigenvectors of $\tilde{A}$ are linearly independent.

The first property is satisfied by any $\tilde{A}$ that looks and feels like a Jacobian; the second property is also easy to obtain. The third property is the critical one, and one which the obvious candidates listed above fail to meet. Properties 3 and 4 are necessary and sufficient to guarantee that the scheme will preserve unchanged exact solutions to the Riemann problem — stationary contact discontinuities and stationary shock waves.

The derivation of this scheme is somewhat complex, so only the result will be presented here. To construct $\tilde{A}$, we must first construct a special average of U_R and U_L called (not surprisingly) the *Roe average*. This average is constructed as follows:

$$\begin{aligned} \tilde{\rho} &= \sqrt{\rho_R \rho_L} \\ \tilde{u} &= \frac{\sqrt{\rho_R} u_R + \sqrt{\rho_L} u_L}{\sqrt{\rho_R} + \sqrt{\rho_L}} \\ \tilde{h} &= \frac{\sqrt{\rho_R} h_R + \sqrt{\rho_L} h_L}{\sqrt{\rho_R} + \sqrt{\rho_L}} \end{aligned} \tag{26}$$

where $h = e + \frac{P}{\rho}$ is the thermodynamic enthalpy per unit mass. Then we can construct $\tilde{A} = A(\tilde{U})$. Properties 1 and 2 are clearly satisfied. Property 4 is satisfied, because the eigenvectors of $A(U)$ are independent for any U. Two of the examples will demonstrate that stationary contact discontinuities are preserved, thus implying that Property 3 is also satisfied.

We can compute fluxes using Roe's scheme with the following procedure:

1. Compute $F_{i+\frac{1}{2};i}$ and $F_{i+\frac{1}{2};i+1}$.
2. Compute $\tilde{U}$ using Equations 26.

3. Compute $|\tilde{A}|$ using Equations 25, 19, 20, 22, and 23. The eigenvalues used in constructing $\left|\tilde{A}\right|$ are computed from $\tilde{U}$

4. Finally, compute $F_{i+\frac{1}{2}}$ using Equation 24.

3.3 Example Problems

Each example was computed using identical meshes with 100 equal-sized control volume, a fourth-order accurate Runge-Kutta time advance scheme, and a second-order accurate limited reconstruction scheme. Each case was run 40 time steps with $\Delta t = 0.005$.

Stationary Contact Discontinuity

The Steger-Warming scheme is clearly deficient for this problem (Figure 4). The initial sharp density jump becomes smeared, and this error is transmitted to the momentum and energy equations, as seen in the variation of velocity and pressure. Roe's scheme (Figure 5) is designed to solve this problem exactly, and does. The only non-zero component of δU is the change in density, and this effect is erased by multiplication with the zero eigenvalue, u. This difference between the two schemes is critical in viscous flow calculations, where Roe's scheme minimizes the cross-stream diffusion compared with Steger-Warming; the latter scheme adds significant and undesirable artificial diffusion into thin shear layers (like boundary layers and wakes). As a consequence, boundary layer velocity profiles are more accurate with Roe's scheme than with Steger and Warming's for equal mesh resolution.

Weak Pressure Waves

Both schemes perform reasonably well in terms of accurately predicting the acoustic wave propagation speed. Again, Roe's scheme does a better job with the stationary contact discontinuity at $x = 0.5$, as seen in density, temperature and velocity profiles in Figures 6 and 7.

Shock Wave Propagation

For this case, (see Figures 8 and 9), the two schemes again produce similar results. Shock propagation speed and shock sharpness are equivalent. The moving contact discontinuity is handled by Roe's scheme without any oscillation in the pressure, which the Steger-Warming

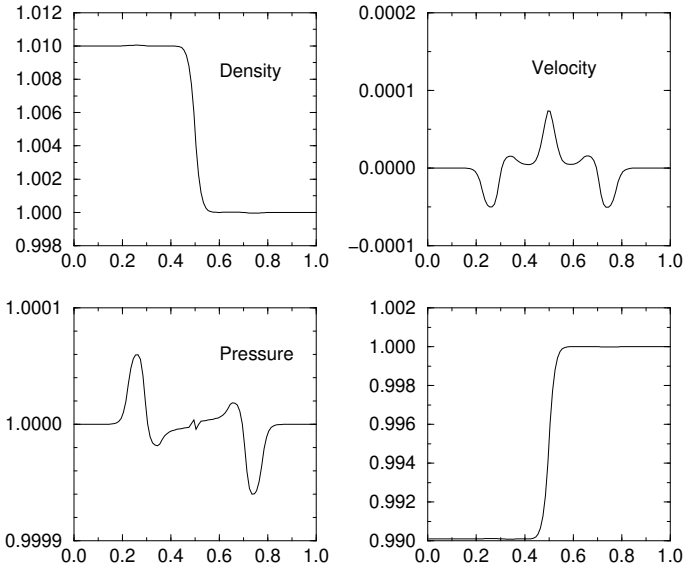

Figure 4: Stationary contact discontinuity using Steger-Warming FVS

scheme produces. Also, careful comparison shows that the contact discontinuity and the expansion fan (especially its foot at about $x = 0.5$) are represented by Roe's scheme with less dissipation.

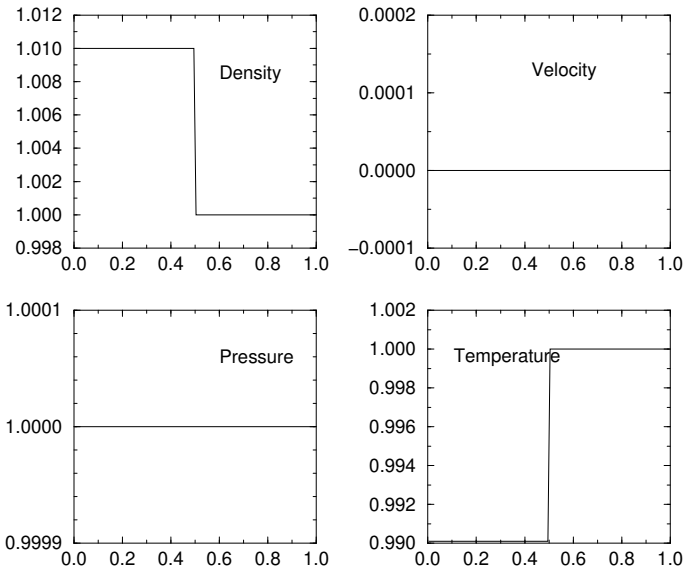

Figure 5: Stationary contact discontinuity using Roe's FDS

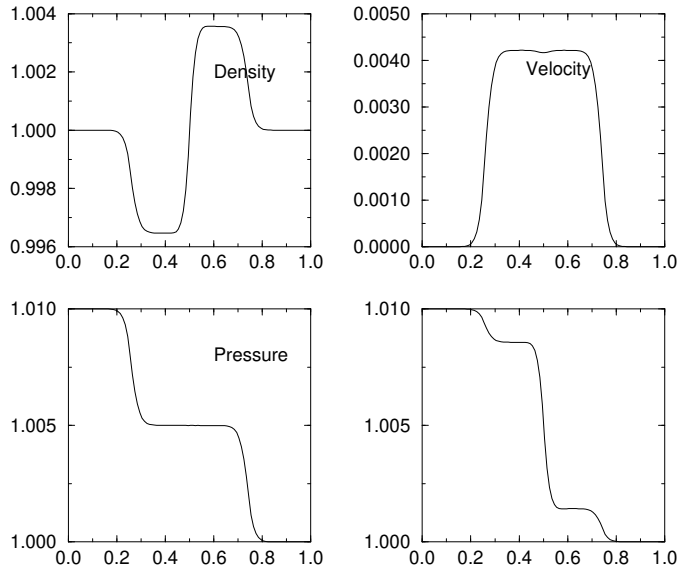

Figure 6: Weak acoustic wave propagation using Steger-Warming FVS

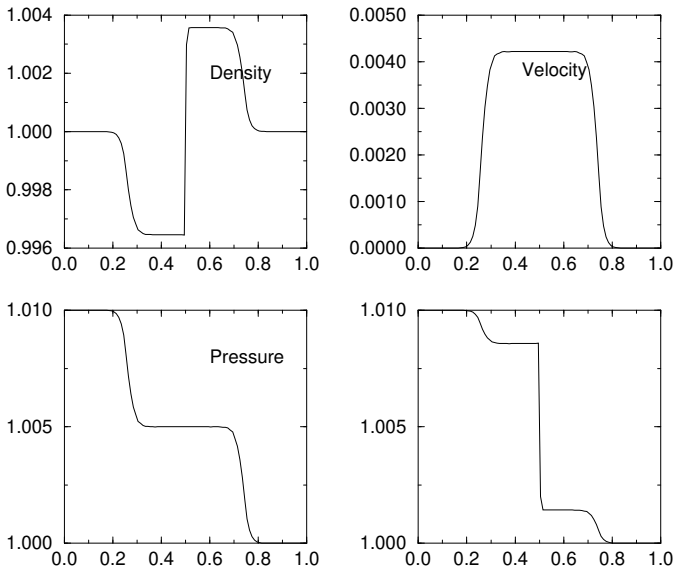

Figure 7: Weak acoustic wave propagation using Roe's FDS

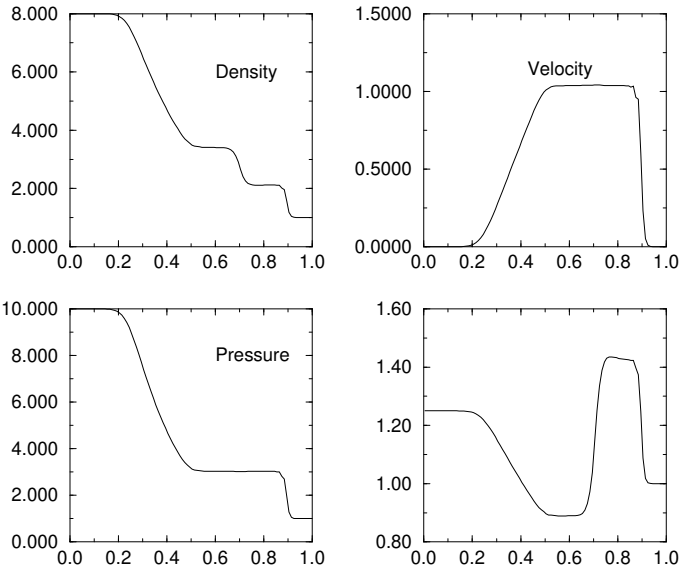

Figure 8: Shock wave propagation using Steger-Warming FVS

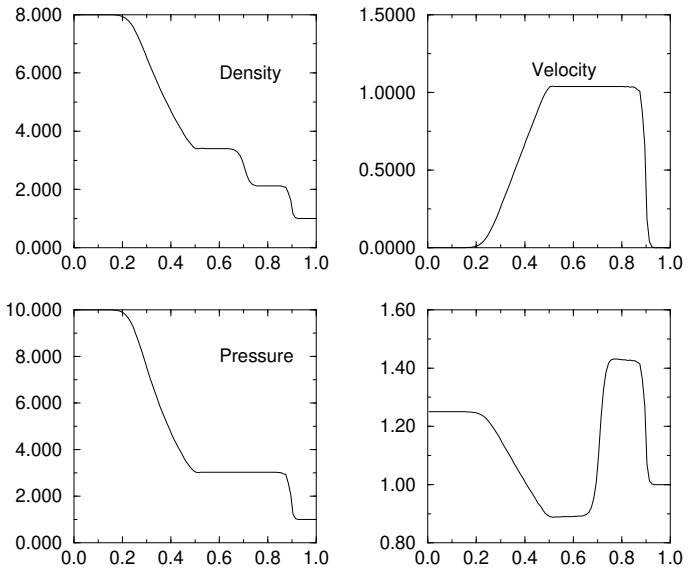

Figure 9: Shock wave propagation using Roe's FDS

3.4 Cautionary Notes

1. The Steger-Warming scheme, as presented, switches abruptly from computing the flux associated with a particular eigenvalue using data on the left of the control volume boundary to data on the right as the associated eigenvalue passes through 0. This behavior is unfortunate, especially with regard to steady-state convergence. A simple fix for this problem is to redefine Λ^+ and Λ^-.

$$\Lambda^+ = \frac{1}{2}\begin{bmatrix} \lambda_1 + \sqrt{\lambda_1^2+\epsilon} & & \\ & \lambda_2 + \sqrt{\lambda_2^2+\epsilon} & \\ & & \lambda_3 + \sqrt{\lambda_3^2+\epsilon} \end{bmatrix}$$

$$\Lambda^- = \frac{1}{2}\begin{bmatrix} \lambda_1 - \sqrt{\lambda_1^2+\epsilon} & & \\ & \lambda_2 - \sqrt{\lambda_2^2+\epsilon} & \\ & & \lambda_3 - \sqrt{\lambda_3^2+\epsilon} \end{bmatrix}$$

   with ϵ generally chosen to be in the range of 10^{-8} or so. This allows a gradual transition from right-side to left-side calculation of fluxes without affecting the total flux computed appreciably.

2. Roe's scheme does an excellent job of preserving shock waves and contact discontinuities because exact solutions of the Rankine-Hugoniot jump conditions for shocks

and contacts are exactly captured by Roe's FDS. Unfortunately, the scheme does not distinguish between entropy-increasing, physically-acceptable compression shocks and entropy-reducing, physically-unacceptable rarefaction shocks. For flows accelerating from subsonic to supersonic Mach numbers, this can cause small glitches in the solution near the sonic point because of rarefaction shocks. This problem is somewhat similar to the Steger-Warming problem just mentioned, in that it occurs because an eigenvalue is too near zero. This can be corrected by redefining $|\Lambda|$ as

$$|\Lambda| = \begin{bmatrix} \sqrt{\lambda_1^2 + \epsilon} & & \\ & \sqrt{\lambda_2^2 + \epsilon} & \\ & & \sqrt{\lambda_3^2 + \epsilon} \end{bmatrix}$$

with a similarly small value of ϵ.

4 Boundary Conditions

4.1 Solid Wall Boundary Conditions

For a finite-volume scheme, the only flux normal to a wall is the flux due to pressure, so $F_{wall} = (0\ P\ 0)$.[6] The pressure is generally obtained by extrapolation. Another alternative is to compute the pressure gradient using the wall-normal component of momentum and to use this to determine pressure at the wall. This is all that is needed for boundary conditions at a wall in inviscid compressible flow.

For viscous compressible flow, appropriate conditions must imposed on temperature and tangential velocity (using ghost cells where necessary). It is generally not necessary to compute the density in the ghost cell, because it is never used for either the viscous or inviscid flux calculation.

4.2 Inflow Boundary Conditions

At an inflow boundary in one dimension, at least two of the three characteristic waves are directed into the domain: the entropy wave (speed u) and the right-running acoustic wave (speed $u + c$). If the flow is supersonic, the (now mis-leadingly named) left-running acoustic wave (speed $u - c$) is also entering the computational domain. This leads to two important cases for inflow boundary conditions.

Note that viscous effects at the inflow and outflow are generally neglected in computing the boundary conditions. While this is not strictly correct in all cases, it is generally an acceptable approximation.

4.2.1 Subsonic Inflow

In this case, two characteristics are entering the domain, so we need two pieces of information from upstream; total pressure P_t and total temperature T_t are commonly used.[7] The third characteristic is leaving the domain, and supplies one piece of information from the interior

[6] All together now: "All you need is P. (dah dah dadadah) All you need is P. (dah dah dadadah) All you need is P. P. P is all you need." Apologies to any who are unfamiliar with the Beatles song *All You Need is Love*, and probably also to the rest, who will never be able to listen to the chorus the same way again.

[7] In two dimensions, a third piece of external data is required. The flow angle is often used. Also, in two dimensions, the effects of the y component of velocity must be considered in Equations 27 and 28, where u^2 must be replaced by $u^2 + v^2$.

of the computational domain. A simple and effective approach for applying such a boundary condition is to use the characteristic information to determine the solution in a ghost cell just outside the computational domain.

In one dimension, we can express the pressure and temperature in terms of total pressure and temperature and the flow velocity:

$$P = P_t \left(1 - \frac{\gamma - 1}{\gamma + 1}\frac{u^2}{c_*^2}\right)^{\frac{\gamma}{\gamma-1}} \tag{27}$$

$$T = T_t \left(1 - \frac{\gamma - 1}{\gamma + 1}\frac{u^2}{c_*^2}\right) \tag{28}$$

$$c_*^2 = 2\gamma\frac{\gamma - 1}{\gamma + 1}C_v T_t$$

These equations give us two relations for P_g, T_g, and u_g for the ghost cell; if we knew the correct value of u_g for the ghost cell, we could compute P_g and T_g. To find u_g, we invoke the characteristic relation for the $u - c$ eigenvalue:

$$\frac{\partial P}{\partial t} - \rho c\frac{\partial u}{\partial t} = -(u - c)\left(\frac{\partial P}{\partial x} - \rho c\frac{\partial u}{\partial x}\right)$$

Suppose we evaluate this using an implicit time differencing scheme and first-order accurate one-sided differences in space. Then, with a small bit of algebra, one can show that

$$\delta P_g - \rho c \delta u_g = \frac{-\lambda_3}{1 - \lambda_3}\left(P_1^n - P_g^n - \rho c\left(u_1^n - u_g^n\right)\right) \tag{29}$$

where $\lambda_3 = (u - c)\frac{\Delta t}{\Delta x}$. But because we can write $P_g = P(u_g)$ (Eq. 27), from differential calculus, we know that

$$\delta P_g = \frac{\partial P}{\partial u}\delta u_g \tag{30}$$

Combining Equations 29 and 30 gives the following expression for δu_g.

$$\delta u_g = \frac{\frac{-\lambda_3}{1-\lambda_3}\left(P_1^n - P_g^n - \rho c\left(u_1^n - u_g^n\right)\right)}{\frac{\partial P}{\partial u} - \rho c}$$

where $\frac{\partial P}{\partial u}$, ρ, λ_3, and c are all evaluated using U_1^n. Given this value for δu_g, one can easily compute u_g^{n+1} and then P_g^{n+1} (Eq. 27), T_g^{n+1} (Eq. 28) and ρ_g^{n+1} (Eq. 4). These values can then be manipulated to compute U_g^{n+1}.

4.2.2 Supersonic Inflow

In this case, all flow data at the boundary is coming from outside the computational domain, and no influence from within the domain can physically propagate out. This makes the boundary condition very simple, with the data in ghost cells set once at the beginning of a run and left unchanged. Both Steger-Warming's and Roe's schemes will use only the upwind data to compute the flux at the boundary of the computational domain.

4.3 Outflow Boundary Conditions

Again, there are two cases to consider: subsonic and supersonic outflow.

4.3.1 Subsonic Outflow

In the subsonic case, two pieces of information for the ghost cell come from the interior and the third from the exterior. The exterior data is nearly always the back pressure at the outflow, P_b. Because this pressure is fixed, the pressure never changes in the ghost cell ($\delta P = 0$).

The two characteristic relations are

$$\begin{aligned} \frac{\partial \rho}{\partial t} - \frac{1}{c^2}\frac{\partial P}{\partial t} &= -u\left(\frac{\partial \rho}{\partial x} - \frac{1}{c^2}\frac{\partial P}{\partial x}\right) \\ \frac{\partial P}{\partial t} + \rho c\frac{\partial u}{\partial t} &= -(u+c)\left(\frac{\partial P}{\partial x} + \rho c\frac{\partial u}{\partial x}\right) \end{aligned}$$

Just as for the inflow boundary, we discretize these conditions using an implicit, first-order scheme.

$$\delta\rho_g - \frac{1}{c^2}\delta P_g = -\frac{\lambda_1}{1+\lambda_1}\left(\rho_g^n - \rho_I^n - \frac{1}{c^2}\left(P_g^n - P_I^n\right)\right) \equiv R_1 \tag{31}$$

$$\delta P_g + \rho c\delta u_g = -\frac{\lambda_2}{1+\lambda_2}\left(P_g^n - P_I^n + \rho c\left(u_g^n - u_I^n\right)\right) \equiv R_2 \tag{32}$$

As for the inflow case, all coefficients are evaluated using U_I^n. Because we already know δP_g, we can easily solve for $\delta\rho_g$ and δu_g. With this information in hand, it is trivial to find U_g^{n+1}.

4.3.2 Supersonic Outflow

In this case, it isn't strictly necessary to compute the solution in the ghost cells. Nevertheless, the approach is presented for completeness. In this case, we add a third characteristic relation

$$\frac{\partial P}{\partial t} - \rho c \frac{\partial u}{\partial t} = -(u - c)\left(\frac{\partial P}{\partial x} - \rho c \frac{\partial u}{\partial x}\right)$$

and discretize it

$$\delta P_g - \rho c \delta u_g = -\frac{\lambda_3}{1 + \lambda_3}\left(P_g^n - P_I^n - \rho c\left(u_g^n - u_I^n\right)\right) \equiv R_3 \tag{33}$$

We can now solve Equations 31, 32, and 33 simultaneously for $\delta\rho_g$, δu_g, and δP_g.

$$\begin{aligned} \delta P_g &= \frac{R_2 + R_3}{2} \\ \delta\rho_g &= R_1 + \frac{\delta P_g}{c^2} \\ \delta u_g &= \frac{R_2 - \delta P_g}{\rho c} \end{aligned}$$

With this information, computing U_g^{n+1} is again trivial.

Further Reading

1. C. Hirsch. *Numerical Computation of Internal and External Flows, Volume 2.* Wiley, 1988. Especially chapters 19 and 20.

2. P. Roe. "Approximate Riemann solvers, parameter vectors, and difference schemes." *J. Computational Physics*, v 43, pp 357–372, 1981.

3. P. Roe. "Characteristic-based schemes for the Euler equations." *Annual Review of Fluid Mechanics,* v 18, pp 337–365, 1986.

4. J. Steger and R. Warming. "Flux vector splitting of the inviscid gasdynamic equations with application to finite-difference methods." *J. Computational Physics*, v 40, pp 263–293, 1981.

5. M.-S. Liou. "A sequel to AUSM: AUSM$^+$." *J. Computational Physics*, v 129, pp 364–382, 1996.